

SIMULATIONS OF RF FIELD-INDUCED THERMAL FEEDBACK IN NIOBIUM AND Nb₃Sn CAVITIES*

Jixun Ding[†], Daniel Leslie Hall, Matthias Liepe

Cornell Laboratory for Accelerator-Based Sciences and Education (CLASSE),
 Ithaca, NY 14853, USA

Abstract

Thermal feedback is a known limitation for SRF cavities made of low-purity niobium, as the increased losses at higher temperature described by BCS theory create a feedback mechanism that can eventually result in a runaway effect and associated cavity quench. In a similar manner, niobium cavities coated with Nb₃Sn may also be subject to increased losses from thermal feedback, as Nb₃Sn is possessed of a much lower thermal conductivity than niobium, although this effect will be mitigated by the thin film nature of the coating. In order to better understand the degree to which thermal feedback plays a role in the performance of Nb₃Sn cavities, it is necessary to understand how the various components of the problem play a role in the outcome. In this paper, we present the first results from simulations performed at Cornell University that model RF induced thermal feedback in both conventional niobium cavities and niobium cavities coated with a thin film of Nb₃Sn. The impacts of layer thickness, niobium substrate thermal conductivity, and trapped flux on the performance of the cavity are discussed.

INTRODUCTION

The effect of RF heating on niobium cavity performance has been studied via the thermal feedback model (TFBM) [1–5]. Heat produced by RF fields at cavity inner surfaces must be transported across a typically 3mm thick layer of niobium and a niobium-Helium interface into liquid Helium. Both niobium and the Nb-He interface have finite thermal conductance, so RF heat production increases the inner surface temperature of a cavity, which in turn increases BCS resistance and heat dissipation, creating a positive feedback loop. At low to moderate fields, the feedback effect is small enough that the temperature inside the cavity reaches a stationary state. The stationary inner surface temperature (and hence surface resistance) can be written as a function of accelerating field strength, which may contribute to the so called “mid-field Q-slope” [5, 6]. Under certain conditions, the feedback mechanism is strong enough that there exists a “thermal breakdown field” H_b , above which no stationary temperature can be sustained [1, 3]. This can manifest as “high field Q-drop” [3] followed by a cavity quench, and is considered the thermal stability limit of a SRF cavity. No work has yet been done to probe the thermal stability limit of niobium cavities coated with Nb₃Sn. To this end, ther-

mal simulations were developed at Cornell University to extend the well established TFBM to apply to Nb₃Sn coated cavities.

SIMULATION METHOD

Bulk Niobium

Our niobium simulations build upon and improve existing HEAT simulations, previously also developed at Cornell [5,7]. We model the cavity wall locally as an infinite slab of niobium and define x as distance from cavity inner surface. The temperature profile in niobium induced by RF heating is shown schematically in Fig. 1. A temperature gradient forms in the cavity bulk, and a temperature jump forms at the Nb-He interface.

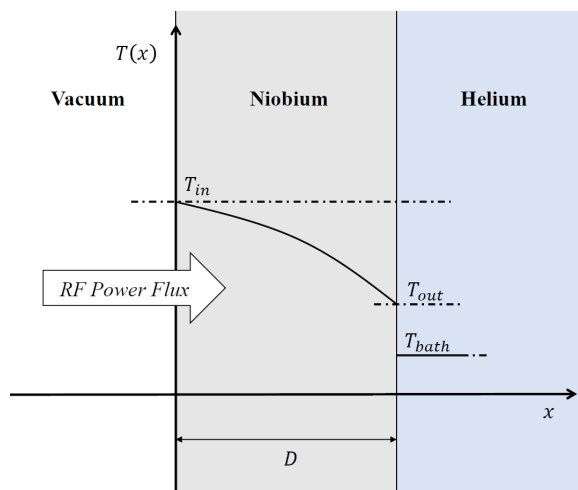


Figure 1: Sketch of steady state temperature profile in niobium.

Using Matlab’s Partial Differential Equation Toolbox [8], we look for a stationary solution $T(x)$ of the one dimensional heat equation

$$\frac{d}{dx} \left(\kappa(T) \frac{dT}{dx} \right) = 0$$

with mixed boundary conditions

$$q = \kappa(T_{in}) \frac{\partial T}{\partial x} \quad \text{at } x = 0 \quad (1)$$

$$q = (T_{out} - T_{bath}) H_k(T_{out}, T_{bath}) \quad \text{at } x = D \quad (2)$$

In the above equations, Eq. 1 defines a Neumann boundary condition and Eq. 2 defines a Dirichlet boundary condition

* This work was primarily supported by U.S. DOE award DE-SC0008431. This work was supported in part by the U.S. National Science Foundation under Award PHY-1549132, the Center for Bright Beams.

[†] jd664@cornell.edu

implicitly. q is heat flux [W/m²] produced by RF heating,

$$q = \frac{1}{2} (R_{BCS}(T_{in}, f) + R_{res}) H_{pk}^2,$$

with the BCS surface resistance $R_{BCS}(T_{in}, f)$ computed by SRIMP [9]. $\kappa(T)$ is the thermal conductivity function of niobium, parameterized by RRR and phonon mean free path (pmfp) [10]. $H_k(T, T_{bath})$ is the Nb-He interface thermal conductivity function, which takes different forms depending on whether T_{bath} is above or below the Helium superfluid transition temperature [2, 11]. R_{res} is residual resistance, f is applied field frequency, H_{pk} is peak applied magnetic field strength, and D is the thickness of the material.

For a given set of physical parameters and an array of applied fields, the simulation finds the stationary temperature solution for each applied field, and produces a Q vs. E_{acc} curve. If it seems from direct calculations that thermal runaway is occurring, we switch to an inverse method, fixing heat flux or temperature at the inner surface, and inferring the applied field via

$$H_{pk} = \frac{2q}{R_{BCS}(T_{in}, f) + R_{res}}.$$

This method allows us to go beyond the low-heat flux solution branch and find the true thermal breakdown field, as described in Refs. [1, 3]. This is not always necessary, as other factors, such as niobium's superheating field and peak nucleate boiling flux (for He I contact), may impose a hard limit on maximum accelerating gradient before thermal breakdown occurs.

It's worth noting that the thermal feedback model is only as good as the parameters and functions we put in. Kapitza conductance for Nb-He II heat transport is still not well understood and a range of reported values exist [11–13]. There is no measurement of Nb-He I heat transport (we make do with Platinum-He I data from Ref. [2]). The SRIMP program calculates linear BCS resistance and does not include any RF field dependency, as it was recently found especially in doped niobium cavities [14–16]. We also currently do not include contributions from the finite electron-phonon energy transfer rate, which results in an additional temperature increase of quasiparticles [15, 16]. In the case of bulk niobium, we do not include any possible weak field dependence of residual resistance. Further development of simulations should allow us to incorporate more refined models of various physical effects.

Nb₃Sn Thin Film Coated Niobium

We apply the same type of analysis to Nb₃Sn coated niobium. In this case, heat generated at the Nb₃Sn inner surface is transported across three layers of material: Nb₃Sn, niobium, and again Nb₃Sn. A typical temperature profile is shown schematically in Fig. 2. Temperature gradients form in each material layer and a temperature jump forms at the Nb₃Sn-He interface. There are two layers of Nb₃Sn, because in the current Cornell vapor diffusion coating procedure,

Nb₃Sn always forms on both the inner and outer surface of the cavity.

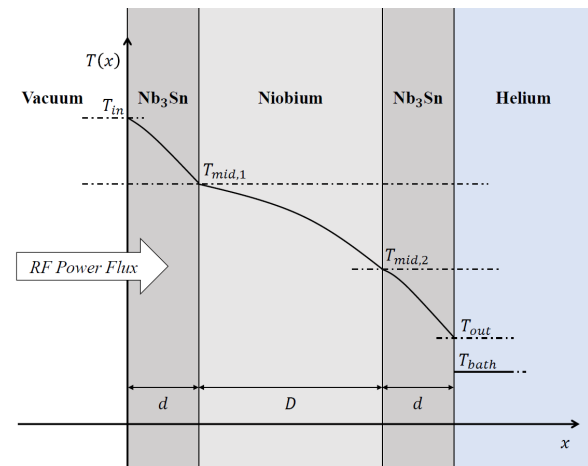


Figure 2: Sketch of steady state temperature profile in Nb₃Sn coated niobium. Thickness of Nb₃Sn layers are greatly exaggerated to make temperature gradients visible.

It is more difficult to model thin film coated niobium numerically, because Nb₃Sn coating layers are usually microns thick, while the niobium substrate is 2 to 3 mm thick. Choosing an appropriate mesh density is difficult if we try to solve the heat equation in three layers of material at once. To get around this problem, we assumed that there is no thermal impedance at Nb-Nb₃Sn interfaces, or equivalently, temperature and heat flux are continuous across metallic boundaries. These assumptions give us sufficient boundary conditions to solve the heat equation in each material layer separately, with appropriate mesh densities and thermal conductivity functions [10, 17], and then connect them together. Since there is no Nb₃Sn-He heat transport data available, we also assumed that Nb₃Sn has the same Kapitza/nucleate boiling behavior as Nb at the helium interface [2, 11]. The Nb₃Sn simulations incorporate the trapped flux sensitivity of Nb₃Sn, $R_{res}(B_{pk})$ [18], instead of using constant R_{res} as in niobium.

RESULTS

Bulk Niobium

We first checked that the simulation gives reasonable agreement with existing niobium performance data, at several different frequencies and temperatures. We compare simulation generated Q vs. E_{acc} curves to four sets of data, two from literature and two from cavity tests performed at Cornell. The comparison is plotted in Fig. 3. For literature data [19, 20] we matched simulation settings to (partially) reported material and cavity geometry parameters [21, 22] as best we could. Default parameter settings were applied to comparison with Cornell ERL data. These settings, as well as common SRIMP settings used by all niobium simulations, are listed in Tables 1 and 2.

Content from this work may be used under the terms of the CC BY 3.0 licence (© 2017). Any distribution of this work must maintain attribution to the author(s), title of the work, publisher, and DOI.

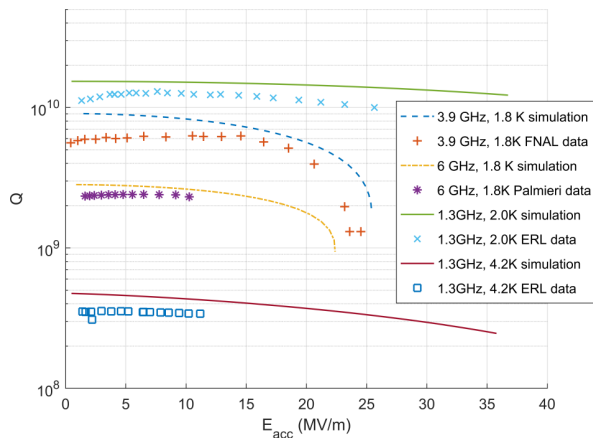


Figure 3: Comparison of simulation generated Q vs. E curves and experimental data from literature [19, 20] and cavity tests at Cornell.

Table 1: List of Material and Geometry Settings

Parameter	Default Value	Ref. [19]	Ref. [20]
R_{res}	10 n Ω	60 n Ω	10 n Ω
RRR	300	300	250
pmfp	50 μ m	1 mm	100 μ m
D	3 mm	2.5 mm	2.6 mm
B_{pk}/E_{acc}	4.08	4.5	4.86
Γ	272	287	275

Table 2: List of Fixed Niobium Parameters for SRIMP

Parameter	Value
T_c	9.2 K
Energy gap	1.92 $\Delta/(k_B T)$
London penetration depth	39 nm
Coherence length	38 nm
Electron mean free path	5 nm

Figure 3 shows that our simulations, even with a few simplifying assumptions, agree with experimental data quite well. In particular, our simulation of 3.9 GHz, 1.8 K cavity performance agrees with similar thermal simulations performed by FNAL, indicating that their cavities are performing near the thermal breakdown limit [23].

Nb₃Sn Thin Film Coated Niobium

The simulation is then used to predict Nb₃Sn cavity performance and evaluate how much RF-field frequency, niobium substrate purity, trapped magnetic flux, and Nb₃Sn coating thickness affect cavity performance. All Nb₃Sn simulations use niobium pmfp = 500 μ m, D = 3 μ m, B_{pk}/E_{acc} = 4.28, and cavity geometry factor Γ = 278. SRIMP settings used to calculate the BCS resistance of Nb₃Sn are listed in Table 3.

As can be seen in Fig. 4, Nb₃Sn cavities at 4.2 K should achieve quality factors comparable to niobium's at 2.0 K.

Table 3: List of Fixed Nb₃Sn Parameters for SRIMP

Parameter	Value
T_c	18 K
Energy gap	2.25 $\Delta/(k_B T)$
London penetration depth	89 nm
Coherence length	7 nm
Electron mean free path	4 nm

At 4.2 K, 1.3 GHz, thermal feedback effects are small, and Q-slope is instead dominated by Nb₃Sn's linearly field dependent residual resistance. In addition, the impact of increased thermal feedback from low substrate niobium RRR is negligible, even at very high fields. This result indicates that pre-anodisation, a technique that improves the uniformity of Nb₃Sn coatings of large cavities while lowering the RRR (and thus thermal conductivity) of the bulk niobium substrate, is not expected to result in significant decreases in performance for 1.3 GHz cavities operating at 4.2 K.

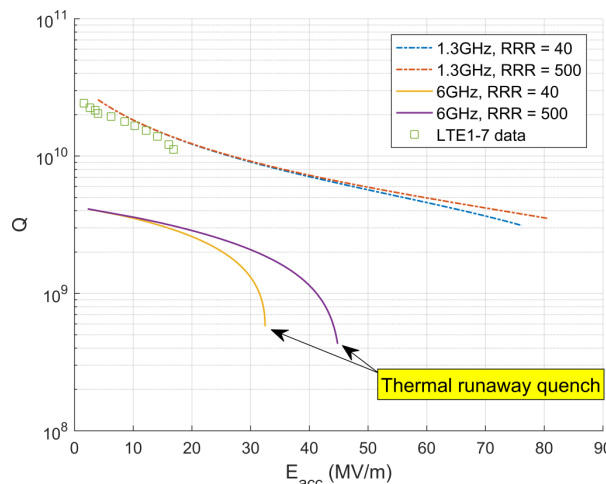


Figure 4: Simulated Q vs. E_{acc} at 4.2 K, for 4 different niobium substrate RRR and frequency settings, compared to cavity test data. Assuming 8 mG of trapped magnetic flux and a coating thickness of 3 μ m.

At 4.2 K, 6 GHz, Q-slope due to thermal feedback is more significant, and high field Q-drop associated with global thermal runaway is visible. Niobium substrate RRR also significantly contributes to thermal feedback at high fields (>25 MV/m). However, the lower intrinsic quality factor ($\sim 3 \times 10^9$) of high frequency operation means that 6 GHz Nb₃Sn cavities might have to be run at lower temperatures, e.g. 2.0 K, at which point we recover high Q ($> 1 \times 10^{10}$), and thermal effects become suppressed due to the exponential temperature dependence of BCS resistance.

Figure. 5 plots impact of Nb₃Sn coating thickness and trapped flux on cavity performance for 4.2 K, 1.3 GHz operation. Due to Nb₃Sn's fairly low BCS resistance at this temperature and frequency setting, residual resistance changes due to flux trapping impacts cavity performance more severely

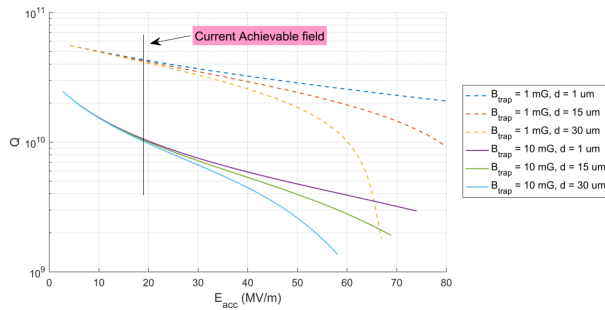


Figure 5: Simulated Q vs. E_{acc} curves at 4.2 K, 1.3 GHz, for 6 different coating thickness and trapped magnetic flux settings. Niobium substrate $RRR = 300$.

than increased thermal feedback from thicker Nb_3Sn coating at current achievable fields (< 18 MV/m [24]). The impact from Nb_3Sn coating thickness becomes significant above 40 MV/m only if the Nb_3Sn layers are thick enough (> 25 μm) to significantly increase inner surface temperature.

CONCLUSION

New thermal simulations developed at Cornell confirm what we know of conventional niobium cavities and can be used to predict thermal stability behavior of Nb_3Sn cavities. At 4.2 K, 1.3 GHz operation, Nb_3Sn thin film coated niobium is not expected to suffer from global thermal feedback at achievable fields, even for reactor grade substrate niobium and thick (~ 30 μm) Nb_3Sn coating layers. These results strongly suggest that other mechanisms are at play in the quenches currently observed at accelerating fields of 15 to 18 MV/m, such as defect induced flux entry or local thermal instability. Residual losses from flux trapping does significantly impact quality factor, placing operational requirements on running Nb_3Sn cavities. Thermal feedback can be a limitation to 6 GHz cavity performance at 4.2 K, suggesting that 6 GHz Nb_3Sn cavities might have to be run at lower temperatures to obtain high enough quality factors, if operation at high fields (e.g. above 20 MV/m) is required.

ACKNOWLEDGEMENT

We would like to thank David Bindel for helpful comments during development of simulation methods.

REFERENCES

- [1] S. Isagawa and K. Isagawa, "Limitations of RF field by thermal breakdown in superconducting niobium cavity," *Cryogenics*, vol. 20, no. 12, pp. 677 – 680, 1980.
- [2] K. Krafft, "Thermal transport and thermal-magnetic breakdown in superconducting cavities made of high thermal conductivity niobium," Ph.D. thesis, Cornell University, Ithaca, USA, 1983.
- [3] A. Gurevich, "Thermal RF breakdown of superconducting cavities," in *Proc. Pushing the Limits of RF Superconductivity Workshop*, Argonne, USA, Sep. 2004, pp. 17 – 25.
- [4] P. Bauer *et al.*, "Evidence for non-linear BCS resistance in SRF cavities," *Physica C: Superconductivity*, vol. 441, no. 1, pp. 51 – 56, 2006.
- [5] J. Vines, Y. Xie, and H. Padamsee, "Systematic trends for the medium field Q-slope," in *Proc. SRF'07*, Beijing, China, Oct. 2007, paper TUP27.
- [6] G. Ciovati and J. Halbritter, "Analysis of the medium field Q-slope in superconducting cavities made of bulk niobium," *Physica C: Superconductivity*, vol. 441, no. 1, pp. 57 – 61, 2006.
- [7] Y. Xie, "Development of superconducting RF sample host cavities and study of pit-induced cavity quench," Ph.D. thesis, Cornell University, Ithaca, USA, 2012.
- [8] MATLAB and Partial Differential Equation Toolbox Release 2016a. Natick, Massachusetts, United States: The MathWorks Inc., 2016.
- [9] J. Halbritter, "Comparison between measured and calculated RF losses in the superconducting state," *Zeitschrift für Physik*, vol. 238, no. 5, pp. 466–476, Oct. 1970.
- [10] F. Koechlin and B. Bonin, "Parametrization of the niobium thermal conductivity in the superconducting state," *Superconductor Science and Technology*, vol. 9, no. 6, p. 453, 1996.
- [11] K. Mittag, "Kapitza conductance and thermal conductivity of copper niobium and aluminium in the range from 1.3 to 2.1 K," *Cryogenics*, vol. 13, no. 2, pp. 94 – 99, 1973.
- [12] J. Amrit and M. X. François, "Heat flow at the niobium-superfluid helium interface: Kapitza resistance and superconducting cavities," *Journal of Low Temperature Physics*, vol. 119, no. 1, pp. 27–40, 2000.
- [13] A. Aizaz, P. Bauer, T. L. Grimm, N. T. Wright, and C. Z. Antoine, "Measurements of thermal conductivity and Kapitza conductance of niobium for SRF cavities for various treatments," *IEEE Transactions on applied superconductivity*, vol. 17, no. 2, pp. 1310–1313, 2007.
- [14] A. Grassellino *et al.*, "Nitrogen and argon doping of niobium for superconducting radio frequency cavities: a pathway to highly efficient accelerating structures," *Superconductor Science Technology*, vol. 26, no. 10, p. 102001, Oct. 2013.
- [15] A. Gurevich, "Reduction of dissipative nonlinear conductivity of superconductors by static and microwave magnetic fields," *Phys. Rev. Lett.*, vol. 113, p. 087001, Aug 2014.
- [16] J. T. Maniscalco, D. Gonnella and M. Liepe, "The importance of the electron mean free path for superconducting radio-frequency cavities," *Journal of Applied Physics*, vol. 121, no. 4, p. 043910, 2017.

- Content from this work may be used under the terms of the CC BY 3.0 licence (© 2017). Any distribution of this work must maintain attribution to the author(s), title of the work, publisher, and DOI.
- [17] G. D. Cody and R. W. Cohen, "Thermal conductivity of Nb₃Sn," *Rev. Mod. Phys.*, vol. 36, pp. 121–123, Jan 1964.
- [18] D. Hall *et al.*, "Field-dependence of the sensitivity to trapped flux in Nb₃Sn," presented at SRF'17, Lanzhou, China, Jul. 2017, paper THPB042, this conference.
- [19] V. Palmieri, A. A. Rossi, S. Y. Stark and R. Vaglio, "Evidence for thermal boundary resistance effects on superconducting radiofrequency cavity performances," *Superconductor Science and Technology*, vol. 27, no. 8, p. 085004, 2014.
- [20] E. Harms, H. Edwards, A. Hocker, T. Khabiboulline and N. Solyak, "Performance of 3.9-GHz superconducting cavities," in *Proc. LINAC'08*, Victoria, BC, Canada, Sep. 2008, paper THP029.
- [21] Rossi *et al.*, "Purification of 6 GHz cavities by induction heating," in *Proc. SRF'13*, Paris, France, Sep. 2013, paper TUIOC05.
- [22] E. Harms *et al.*, "Status of 3.9-GHz superconducting rf cavity technology at Fermilab," in *Proc. LINAC'06*, Knoxville, Tennessee USA, Aug. 2006, paper THP051.
- [23] E. Harms *et al.*, "Status of 3.9 GHz superconducting rf cavity technology at Fermilab," in *Proc. SRF'07*, paper WEP41.
- [24] D. Hall, J. Kaufman, M. Liepe, R. Porter, and J. Sears, "First results from new single-cell Nb₃Sn cavities coated at cornell university," in *Proc. IPAC'17*, Copenhagen, Denmark, May 2017, paper MOOCA2.